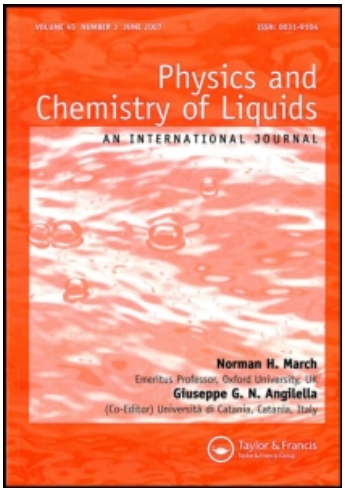

Physics and Chemistry of Liquids
Publication details, including instructions for authors and subscription information:
http://www.informaworld.com/smpp/title~content=t713646857

An Ionic Model for Molecular Units in Molten Aluminium Trichloride and Alkali Chloroaluminates

Z. Akdeniz[a]; G. Pastore[b]; M. P. Tosi[c]
[a] Physics Department, University of Istanbul, Istanbul, Turkey and International Centre for Theoretical Physics, Strada Costiera 11, Trieste, Italy [b] Istituto Nazionale di Fisica della Materia and Dipartimento di Fisica Teorica, Università di Trieste, Trieste, Italy [c] Istituto Nazionale di Fisica della Materia and Classe di Scienze, Scuola Normale Superiore, Pisa, Italy

To cite this Article Akdeniz, Z. , Pastore, G. and Tosi, M. P.(1996) 'An Ionic Model for Molecular Units in Molten Aluminium Trichloride and Alkali Chloroaluminates', Physics and Chemistry of Liquids, 32: 4, 191 — 209
To link to this Article: DOI: 10.1080/00319109608030534
URL: http://dx.doi.org/10.1080/00319109608030534

Phys. Chem. Liq., 1996, Vol. 32, pp. 191–209
Reprints available directly from the publisher
Photocopying permitted by license only

AN IONIC MODEL FOR MOLECULAR UNITS IN MOLTEN ALUMINIUM TRICHLORIDE AND ALKALI CHLOROALUMINATES

Z. AKDENIZ[1], G. PASTORE[2] and M. P. TOSI

[1]*Physics Department, University of Istanbul, Istanbul, Turkey and International Centre for Theoretical Physics, Strada Costiera 11, I-34014 Trieste, Italy*
[2]*Istituto Nazionale di Fisica della Materia and Dipartimento di Fisica Teorica, Università di Trieste, I-34014 Trieste, Italy*
[3]*Istituto Nazionale di Fisica della Materia and Classe di Scienze, Scuola Normale Superiore, I-56126 Pisa, Italy*

(Received 10 February 1996)

A simple ionic model including anion polarizability is developed for the Al_2Cl_6 molecular dimer and is tested against data on bond lengths, bond angles and vibrational frequencies from experiment and from molecular orbital calculations. The transferability of the model is tested through calculations of structure and vibrational frequencies for the $(AlCl_4)^-$ and $(Al_2Cl_7)^-$ molecular ions as well as for related ionic clusters, the results being compared with available data. Further calculations are reported showing that the Al_2Cl_6 dimer is strongly stable against fluctuations into ionized states, the fluctuations examined being chlorine exchange between neighbouring dimers and the appearance of ionized products at intermediate stages in the dissociation of the dimer into neutral monomers. The relevance of the results to theoretical understanding of molten chloroaluminates in the acidic range up to pure molten $AlCl_3$ is discussed.

Keywords: Molten salts; molecular dimers.

1. INTRODUCTION

Molten alkali haloaluminates represented by the formula $(AX)_{1-x}$ $(AlX_3)_x$, where A is an alkali and X is chlorine or bromine, provide a striking example of systems in which the stability and coexistence of different complex anions in the melt depend strongly on its composition (for a recent brief review see Tosi, Price and Saboungi [1]). Various evidence from Raman and infrared spectroscopy [2–4], thermodynamic measurements [5–7]

X-ray and neutron diffraction [8 – 14] and molecular dynamics calculations [15 – 17] supports the view that, while the stoichiometric mixture at $x = 0.5$ is composed of alkali ions and tetrahedral $(AlX_4)^-$ anions, the species $(AlX_4)^-$, $(Al_2X_7)^-$, $(Al_3X_{10})^-$ and Al_2X_6 coexist in acidic melts ($0.5 < x < 1$) in proportions which vary with the overall composition. The larger complex anions are formed by $(AlX_4)^-$ tetrahedra sharing corners, while Al_2X_6 consists of two tetrahedra sharing an edge.

At the end of the acidic composition range, pure $AlBr_3$ melts from a crystalline structure which may be described as built from dimeric Al_2Br_6 units with the bromines forming a nearly perfect hexagonal close packing and the Al ions occupying tetrahedral sites [18]. Raman scattering data [4] and neutron diffraction data [13] are consistent with the Al_2Br_6 units being still the dominant species in molten $AlBr_3$. On the contrary, the crystal structure of $AlCl_3$ is formed from a slightly distorted cubic close packing of chlorines, within which the Al ions occupy every second plane of octahedral sites [19]. There is general consensus that on melting the coordination of the Al ions changes from octahedral to essentially tetrahedral. A cooperative transition of the assembly of Al ions between these two types of sites in the $AlCl_3$ crystal would lead to the formation of dimeric Al_2Cl_6 units as basic constituents [20]. The view that melting of $AlCl_3$ yields a molecular liquid of correlated Al_2Cl_6 dimers was proposed a long time ago on the basis of X-ray diffraction data [8] and is consistent with the relatively low melting temperature and the truly enormous changes in molar volume and entropy on melting [7], with Raman scattering data and *ab initio* calculations of vibrational frequencies [4], with the extremely low electrical conductivity of the melt [1], (down by factors of 10^7 on molten NaCl and of 2000 on molten $ZnCl_2$) and with its low shear viscosity [1] (down by factors of 3 on molten NaCl and of 10^4 on molten $ZnCl_2$). Of course, in the melt at $x = 1$ an appreciable amount of corner sharing between tetrahedra such as in $(Al_2X_7)^-$ would require the presence of positively charged units, in conflict with the dominant fourfold coordination of the Al ions.

Further microscopic details on the liquid structure of alkali haloaluminates at selected compositions have emerged from recent neutron diffraction experiments. Blander *et al.* [12] have examined molten KAl_2X_7 and KAl_3X_{10} with X = Cl and Br and discussed their data with the help of information on the geometry of complex anions from quantum chemical calculations. Their main finding, in addition to tetrahedral coordination of Al ions by halogens and a rather close-packed arrangement of the halogens, is the presence of a first sharp diffraction peak (FSDP) signalling the presence of intermediate range order in the melt. This structural feature is

primarily associated with the distribution of the Al ions in space [21], but unfortunately the relative weighting factor of the Al-Al structure factor is only at the level of a percent. The FSDP is observed in the total neutron diffraction patterns only through ghosts in the Al-X and X-X partial structure factors. The FSDP is now known to be present also in the neutron diffraction pattern of several pure molten trihalides, including $AlBr_3$ [13] and $AlCl_3$ [14].

Badyal *et al.* [14] have examined by neutron diffraction the systems $(ACl)_{1-x}(AlCl_3)_x$ with A = Li and Na at various compositions in the range $0 \leqslant x \leqslant 1$. The observed behaviour of the FSDP with increasing concentration of alkali chloride indicates progressive reduction in connectivity and in the length scale of intermediate range order as the concentration of $(AlCl_4)^-$ units increases. Equally good fits of the data on pure molten $AlCl_3$ are obtained by reverse Monte Carlo simulation for very different values of the Al-Al bond length, as a consequence of the negligible weight of the Al-Al structure factor in the total neutron diffraction pattern. Yet the analysis yields a proportion of corner sharing to edge sharing arrangements of $(AlCl_4)^-$ tetrahedra which is crucially dependent on the assumed value of this bond length.

Evidently the Al-Al correlations are the most characterizing structural aspect of these melts, but are as yet not available from experiment. The predictions on these correlations from molecular dynamics computations [15 – 17] are extremely sensitive to the underlying model for the ionic interactions. Thus Saboungi *et al.* [17] report that the predicted value of the Al-Al bond length in a model simulating $NaAlCl_4$ drops from 4.6 Å to 2.5 Å on allowing for polarization of the chlorines through linear response to the local electric field. They also remark that within an ionic model the formation of the double-bridged Al_2Cl_6 species results from the stabilization of bent Al-Cl-Al triplets relative to linear triplets and this is crucially dependent on halogen polarizability. In a variety of halide molecular systems polarization provides a compensating mechanism to stabilize a bent molecular configuration against the increase of the Coulomb repulsion of the halogen ions under bending [22].

An attempt at a refined quantitative model for the ionic interactions in haloaluminates seems justified in the light of the evidence that we have summarized above. This is the main aim of the present work. Halogen polarizability must evidently be included in the model, but a linear electrostatic treatment overemphasizes its role as explicitly noticed by Saboungi *et al.* [17]. As in earlier work on tetrahedral anions [23], we include the counterbalancing effects of overlap deformability of the electronic shells of

the ions through a suitable adaptation of the shell model which was developed in the sixties in connection with the theory of lattice dynamics in ionic crystals [24]. At least for alkali halides this approach has received a quantum mechanical justification from exchange perturbation theory. [25–26] The model that we develop is adjusted to Al-Cl bond lengths in $(AlCl_4)^-$ and in Al_2Cl_6, the number of adjustable parameters being kept minimal by their assumed transferability. The model is then tested in a variety of other calculations of molecular properties for these and other relevant molecular groups, through comparisons with data from experiment and from quantum chemical calculations.

2. METHOD

We present in this section our model for the potential energy U of a molecular unit of arbitrary shape and a brief description of a simple computer programme which is designed to perform two basic functions, namely (i) the optimization of a given starting configuration of an atomic cluster by minimization of its potential energy towards states of static (stable or unstable) equilibrium and (ii) the study of static and dynamic deformations of the cluster for the evaluation of its vibrational frequencies and of its dynamical evolution at constant total energy.

The potential energy U is a function of the interionic vector distances $\mathbf{r}_{ij}$ and of the electric dipole moments $\mathbf{p}_i$ carried by the ions. It consists in our model of the sum of six terms, namely

$$U = U_{cc} + U_r + U_W + U_{cd} + U_{dd} + U_{sm} \tag{2.1}$$

where the various contributions are, in order, the charge-charge interaction energy, the interionic overlap repulsive energy, the van der Waals energy, the charge-dipole interaction energy, the dipole-dipole energy and the overlap-deformability (shell-model) energy. Since the polarizability of Al^{3+} is completely negligible compared to that of Cl^-, the van der Waals interactions and the induced electric dipoles are restricted to the halogens.

The specific expressions for the terms in Eqn. (2.1) are as follows:

$$U_{cc} = \frac{1}{2}e^2 \sum_{i \neq j} \frac{Z_i Z_j}{r_{ij}} \tag{2.2}$$

with Z_i the conventional integral ionic valences;

$$U_r = \sum_{i \neq j} \Phi_{ij}(r_{ij}) \tag{2.3}$$

with the function $\Phi_{ij}(r)$ written in the form proposed by Busing, [27]

$$\Phi_{ij}(r) = f(\rho_i + \rho_j) \exp[(R_i + R_j - r)/(\rho_i + \rho_j)] \tag{2.4}$$

in terms of ionic radii R_i and ionic shell-stiffness parameters ρ_i;

$$U_W = -\frac{1}{2} \sum_{i \neq j} \frac{C_i C_j}{r_{ij}^6}, \tag{2.5}$$

with the double sum running over the halogens only as already remarked;

$$U_{cd} = -\sum_{i \neq j} Z_i e \frac{\mathbf{p}_j \cdot \mathbf{r}_{ij}}{r_{ij}^3} \tag{2.6}$$

with the sum over j running over the halogens only;

$$U_{dd} = \frac{1}{2} \sum_{i \neq j} \left[\frac{\mathbf{p}_i \cdot \mathbf{p}_j}{r_{ij}^3} - 3 \frac{(\mathbf{p}_i \cdot r_{ij})(\mathbf{p}_j \cdot r_{ij})}{r_{ij}^5} \right] + \frac{1}{2\alpha} \sum_j p_j^2, \tag{2.7}$$

with α the polarizability of Cl^- and all sums running over the halogens only; and

$$U_{sm} = \frac{Y}{\alpha K} \sum_{i,j} \frac{\mathbf{p}_j \cdot \mathbf{r}_{ij}}{r_{ij}} \left| \frac{d\Phi_{ij}(r_{ij})}{dr_{ij}} \right|, \tag{2.8}$$

the sum over i being restricted to the metal ions and that over j to the halogens.

On minimizing the energy with respect to the dipoles it is easily realized that the equilibrium value of the dipole on each halogen in an arbitrary configuration of the ionic cluster is the sum of a term proportional to the local electric field and of a counteracting deformation dipole due to the overlap deformability of the valence electron shell of the halogen. The deformation dipole is the sum of contributions arising from overlap with the neighbouring metal ions, each of these being directed along the Al-Cl bond and pointing towards the metal ion.

The expressions (2.1)–(2.8) involve a number of parameters. A first assessment of their values for the molecular units of present interest can be obtained from the work of Wang Li and Tosi [23], who combined earlier estimates in the literature with trends displayed by polyvalent metal halides and with an assumed value of 2.15 Å for the Al-Cl bond length in $(AlCl_4)^-$ (values for this bond length in the literature [12] are in the ranges 2.11–2.16 Å from experiment and 2.15–2.17 Å from molecular orbital calculations). The results of Wang Li and Tosi are reported as WT in the first row of Table I. The second and third row in Table I give a refined assessment of these parameters that we have obtained by fitting the structure of the chlorine bridge in Al_2Cl_6, in a manner that will be described in more detail in the following section. The main point to be noticed here is that the chlorine bridge is very sensitive to the model used for the electric dipoles in the molecule, as anticipated in the introduction, and that its structure can be accurately reproduced only by an appreciable decrease of the chlorine polarizability α relative to the value estimated by Wang Li and Tosi.

We finally turn to describe the computer programme used in the calculations that will be presented below. For both purposes mentioned earlier, namely the search of static equilibrium structures and the evaluation of the vibrational frequencies in a cluster, the general expression of the potential energy is used to evaluate the force acting on each ion of the cluster in an arbitrary configuration. The simplest structure-determination algorithm uses a constant-step steepest descent, evaluating the α-th Cartesian coordinate $x_{i\alpha}$ of the i-th ion at the $(n+1)$ iteration from

$$x_{i\alpha}^{(n+1)} = x_{i\alpha}^{(n)} + \delta F_{i\alpha}[x^{(n)}]. \tag{2.9}$$

Here, $F_{i\alpha}[x^{(n)}]$ is the α-th Cartesian component of the force acting on the i-th ion after the n-th step and δ is a suitably chosen parameter such that the potential energy steadily decreases through the series of iterations. Although this algorithm is in no way the most efficient [28], it is very simple and is adequate for our purposes. Notice that such a local minimization

TABLE I Interionic force parameters (M denotes Al^{3+} and X denotes Cl^-)

	f $(e^2/\text{Å}^2)$	R_M (Å)	ρ_M (Å)	R_X (Å)	ρ_X (Å)	C_X $(e\text{Å}^{5/2})$	α (Å^3)	Y/K (Å$^{3/2}/e$)
WT	0.05	1.05	0.0565	1.71	0.238	5.5	3.0	0.83
PX_1	0.05	1.055	0.049	1.71	0.238	5.5	2.05	0.46
PX_2	0.05	1.06	0.0525	1.71	0.238	5.5	1.91	0.465

algorithm just searches for the local zero-force structure which is nearest to the starting configuration. As we shall see for $(Al_2Cl_7)^-$ it yields the stable structure as well as a multiplicity of saddle-point structures in configuration space.

The determination of vibrational frequencies is next carried out by numerical diagonalization of the full dynamical matrix as obtained by numerical differentiation of the forces acting on the atoms near their equilibrium positions. A saddle-point structure is identified at this step from having one or more imaginary frequencies.

In addition to performing the above static calculations the programme can follow the dynamic evolution of the cluster by means of molecular dynamics using the simple Verlet algorithm,

$$x_{i\alpha}^{(n+1)} = 2x_{i\alpha}^{(n)} - x_{i\alpha}^{(n-1)} + m_i^{-1}(dt)^2 F_{i\alpha}[x^{(n)}], \tag{2.10}$$

where m_i is the ionic mass and dt is the integration time step. This is chosen so as to keep the total energy constant within a small fraction (typically less than one thousandth) of the fluctuations in potential energy. Additional equilibrium structures of the cluster are searched by these means, in the spirit of the strategy of dynamic simulated annealing [29].

With both static and dynamic algorithms the evolution of the cluster is in general unconstrained. However, in some cases a constraint may be needed for the specific purpose of studying a cluster in a non-equilibrium configuration and can be most simply introduced by a suitable modification of the forces. For instance we shall describe below a calculation on the dissociation path of Al_2Cl_6, in which several molecular shapes were evaluated at various fixed (non-equilibrium) values of the Al-Al bond length. This constraint was realized by setting to zero the forces acting on the two metal ions at each value of their separation.

3. EQUILIBRIUM STRUCTURE OF THE Al_2Cl_6 DIMER

The structure of the Al_2Cl_6 dimer at equilibrium is shown in Figure 1. Table 2 reports the calculated bond lengths and bond angles and compares them with data from electron diffraction measurements in the vapour [30] and with results of quantum chemical calculations (QCC) [4]. The notations Cl^B and Cl^T have been used to denote a bridging chlorine and a terminal chlorine, respectively.

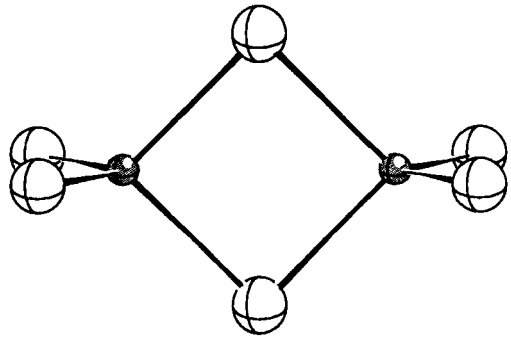

FIGURE 1 Stick-and-ball model of Al_2Cl_6, built with the equilibrium values of the structural parameters evaluated in the PX_1 ionic model.

TABLE II Equilibrium structure of Al_2Cl_6 (bond lengths in Å, bond angles in degrees). Values in parentheses have been fitted to the diffraction data on the Al_2Cl_6 vapour

	$Al\text{-}Cl^B$	$Al\text{-}Cl^T$	$Al\text{-}Al$	$Cl^B\text{-}Cl^B$	$Cl^T\text{-}Cl^T$	$Cl^B\text{-}\hat{A}l\text{-}Cl^B$	$Cl^T\text{-}\hat{A}l\text{-}Cl^T$
WT	2.258	2.076	3.07	3.31	3.58	94.4	119.4
PX_1	2.268	(2.065)	3.22	3.19	3.60	89.5	121.3
PX_2	2.279	2.070	3.28	(3.16)	3.61	87.8	121.6
Expt [30]	2.252	2.065	3.21	3.16	3.64	91.0	123.4
QCC [4]	2.289	2.083	3.26	3.21	3.64	89.1	121.8

The first row in Table II reports the results that we have obtained by means of the WT parameters for the interionic forces. This model, which as already recalled is adjusted to reproduce an approximate value of 2.15 Å for the Al-Cl bond length in the tetrahedral $(AlCl_4)^-$ molecular ion, yields already rather good values for the two Al-Cl bond lengths in Al_2Cl_6.

However, it underestimates the Al-Al bond length by 0.1 – 0.2 Å and correspondingly overestimates the distance between the two bridging chlorines. This defect arises from the same cause as we have already recalled in § 1 in connection with the simulation work of Saboungi *et al.*, [17] i.e. from an overestimate of the polarization dipoles induced on the bridging chlorines. It is quantitatively mitigated in our model by our account of the counteracting deformation dipoles, but is not wholly cured when the WT value of the halogen polarizability is adopted. Incidentally, by wholly omitting halogen polarization we would get the exceedingly large value of 3.83 Å for the Al-Al bond length, stressing again the role of polarizability in parallel with the work of Saboungi *et al.* [17]

We have next readjusted the WT model parameters, and primarily the chlorine polarizability, in two alternative ways, i.e. either by optimizing the values of the Al-Cl^T and Al-Al bond lengths in Al_2Cl_6 in comparison with experiment or by fitting the measured value of the Cl^B-Cl^B bond length. The two procedures yield very similar values for the model parameters, which are reported in Table I as PX_1 and PX_2, respectively. The corresponding results for the equilibrium structure of the Al_2Cl_6 dimer are reported in the second and third row of Table II. It can be seen that in either case the quality of our results in comparison with experiment is comparable to that of the available quantum chemical calculations.

In correspondence with the equilibrium structure we have obtained values of 102.7 eV in the PX_1 model and of 101.3 eV in the PX_2 model for the energy needed to break the Al_2Cl_6 molecule into its atomic constituents in the ionized state. These values are to be compared with a value of about 110 eV as may be estimated from standard data on heats of formation, ionization potentials and electron affinities [31].

All the calculations to be reported below will be based on the PX_1 model, except where explicitly noted. We stress again that this model embodies a fit of the approximately known values of the Al-Cl bond length in $(AlCl_4)^-$ and of the Al-Cl^T bond length in Al_2Cl_6. It is seen from Table II that it yields a value of the Al-Al bond length in Al_2Cl_6 which is in very close agreement with experiment. Our next task will be to test the transferability of this model by calculations on the equilibrium structures of the $(Al_2Cl_7)^-$ complex anion and of other ionic clusters which may be of interest in connection with molten chloroaluminates.

4. STRUCTURE OF COMPLEX IONS AND OF THE $AlCl_3$ MOLECULE

4.1. Structure of $(Al_2Cl_7)^-$

It is known from *ab initio* [32] and semi-empirical [4, 33] molecular orbital calculations that the $(Al_2Cl_7)^-$ complex anion is formed by two $AlCl_4$ tetrahedra sharing a chlorine in a bent configuration with an Al-$\hat{Cl}^B$-Al angle of about 130°. Four such corner-bridged structures, which essentially differ only for internal rotations giving different relative orientations to the two triplets of terminal chlorines, are shown in Figure 2. The C_s (top left, after turning sideways) and C_{2v} (top right) configurations have a 'staggered' and an 'eclipsed' arrangement of the two $AlCl_3$ groups, respectively. The C_2 configuration (bottom left) is obtained from the C_{2v} one by rotation of the

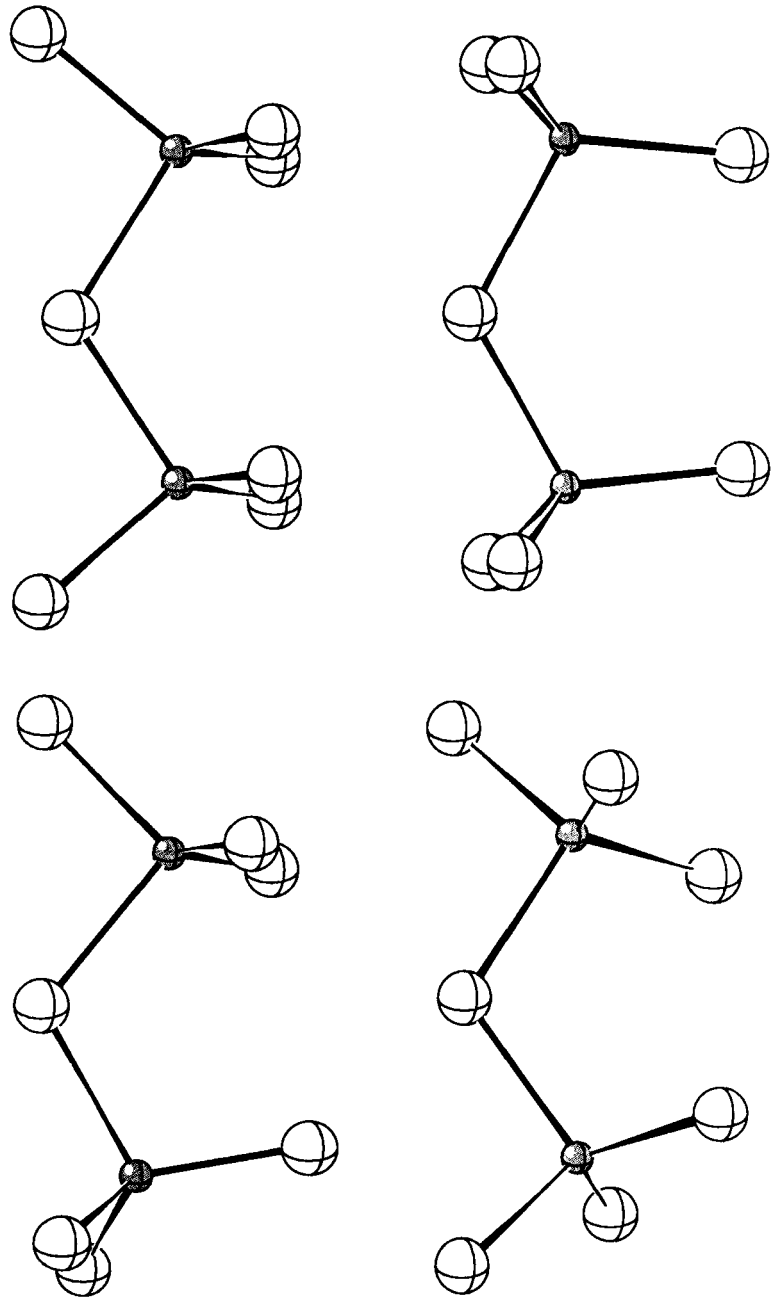

FIGURE 2 Stick-and-ball models of $(Al_2Cl_7)^-$, built with equilibrium values of the structural parameters evaluated in the PX_1 ionic model. From top left to bottom right (after turning the drawing sideways) are shown the C_s, C_{2v}, C_2 and C'_{2v} structures.

two $AlCl_3$ groups around the respective Al-Cl^B bonds by 30° in opposite directions, while the fourth configuration (here denoted by C'_{2v}, bottom right) is similarly obtained by means of rotations by 180°.

The *ab initio* calculations carried out by Curtiss [32] at the Hartree-Fock level have shown that all the above configurations of $(Al_2Cl_7)^-$ are almost degenerate in energy. More precisely, the C_s and C_2 configurations are at essentially the same energy while the two C_{2v} configurations are higher in energy by a few to several tenths of a kcal/mol. In their semi-empirical molecular orbital calculations Blander *et al.* [4] have instead reported the C_2 configuration as being lowest in energy.

In our model a bent corner-sharing configuration for $(Al_2Cl_7)^-$ is stabilized against a linear bridge by the specific inclusion of chlorine polarizability. Static linear structures are found to be about 0.5 eV higher in energy and turn out to be unstable against bending in our calculations of vibrational modes. Edge-sharing and face-sharing structures are found at still higher energies and again are dynamically unstable. All the four bent corner-sharing configurations which are shown in Figure 2 are obtained in our model as structures in static equilibrium, with the C_2 configuration lying at the lowest energy (−106.15 eV relative to separated ions). The C_s, C_{2v} and C'_{2v} structures lie in this order at slightly higher energies and are all unstable against small deformations leading them into the C_2 structure. Thus the C_2 configuration is according to our model the true equilibrium structure of the $(Al_2Cl_7)^-$ anion, while all the other structures correspond to a multiplicity of saddle points separating several equivalent energy minima for the molecular ion in the C_2 structure in a rather complex energy-configuration landscape.

Our results for bond lengths and bond angles of $(Al_2Cl_7)^-$ in the C_2 and C_s structures are shown in Table III, together with the results reported by

TABLE III Theoretical results for the C_2 and C_s structures of $(Al_2Cl_7)^-$ (bond lengths in Å, bond angles in degrees). The two bottom rows report results obtained by Curtiss [32] for the C_s structure from molecular orbital calculations with two different basis sets. The ranges of values shown for bond lengths and bond angles span those appropriate to inequivalent terminal chlorines

	$Al\text{-}Cl^B$	$Al\text{-}Cl^T$	$Al\text{-}\hat{C}l^B\text{-}Al$	$Cl^T\text{-}\hat{A}l\text{-}Cl^B$
$C_2(PX_1)$	2.32	2.10–2.12	111	99–108
$C_2(PX_2)$	2.33	2.10–2.12	113	100–107
$C_s(PX_1)$	2.32	2.10–2.12	112	97–109
C_s(STO–3G)	2.24	2.086–2.089	133.6	103.9–105.6
C_s(3–21G)	2.37	2.200–2.203	131.6	103.3–105.2

Curtiss [32] for the anion in the C_s structure with two different basic sets denoted by STO-3G and 3–21G. His calculated bond lengths show strong sensitivity to the choice of the basis set and, while the values from the 3–21G basis set correspond to a deeper minimum in the molecular energy, the same 3–21G set overestimates the Al-Cl bond length in $(AlCl_4)^-$ by almost 0.1 Å [34]. Semi-empirical molecular orbital calculations on the C_2 structure [4,33] have yielded a value of 2.30 Å for the Al-Cl^B bond length and values of 124.9°–125.8° for the Al-$\hat{Cl}^B$-Al bond angle.

On the above grounds we feel that our results for the Al-Cl bond lengths in $(Al_2Cl_7)^-$ are not only consistent with the available results from quantum chemical calculations, but also of rather good quality. On the other hand, our calculations seem to underestimate the Al-$\hat{Cl}^B$-Al angle by 15°–20°, implying that the Al-Al bond length may be underestimated by as much as 0.2 Å. A further reduction of the chlorine polarizability in the PX_1 model to values in the range 1.3–1.4 $Å^3$ leaves the Al-Cl^B bond length essentially unchanged, increases the Al-Cl^T bond lengths to 2.15–2.16 Å and yields essential agreement with the quantum chemical calculations for the bond angles.

It thus appears that at the present level of accuracy our model may yield useful though not fully quantitative predictions on ionic clusters other than those on which it has been adjusted. Further refinements can be made with the help of improved quantum chemical studies of the equilibrium structure of $(Al_2Cl_7)^-$.

4.2. Structure of $(Al_2Cl_5)^+$

We next evaluate the equilibrium structure of the $(Al_2Cl_5)^+$ complex cation and hence the energy required for the ionization reaction

$$2(Al_2Cl_6) \rightarrow (Al_2Cl_7)^- + (Al_2Cl_5)^+ \qquad (4.1)$$

in vacuo.

Our results for the structure of the $(Al_2Cl_5)^+$ ion are shown in Figure 3 and in Table IV. Relative to Al_2Cl_6, the Cl^B-$\hat{Al}$-Cl^B angle is increased from 89.5° to 96° for the threefold-coordinated Al ion and decreased to 84° for the fourfold-coordinated one. The corresponding Al-Cl^B bond lengths are respectively decreased and increased by about 0.1 Å, as shown in Table IV. It is also seen from Table IV that the Al-Cl^T bond lengths are only slightly decreased relative to that given in Table II for Al_2Cl_6.

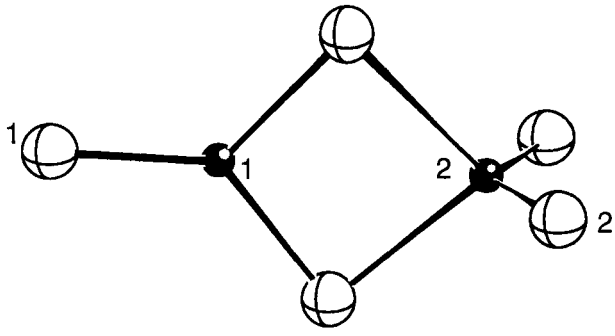

FIGURE 3 Stick-and-ball model of $(Al_2Cl_5)^+$, built with the equilibrium values of the structural parameters evaluated in the PX_1 ionic model.

TABLE IV Equilibrium bond lengths in $(Al_2Cl_5)^+$ (in Å)

	Al_1-Cl^B	Al_2-Cl^B	Al_1-Cl_1^T	Al_2-Cl_2^T
PX_1	2.13	2.40	2.00	2.03

The extraction of a terminal chlorine from Al_2Cl_6 is thus accompanied by relatively small readjustments of the remaining ions. Nevertheless the molecular ground state energy increases by a very sizable amount, from -102.7 eV to -93.9 eV relative to independent ions. Combining these values with our result for the ground state energy of $(Al_2Cl_7)^-$, which is -106.1 eV, we estimate that the reaction in Eqn. (4.1) requires an energy expense of 5.4 eV. A gain of anion-cation Coulomb interaction energy of this magnitude may be expected in a dense phase only for small-sized monovalent ions. We conclude that ionic fluctuations associated with anion transfer between neighbouring Al_2Cl_6 molecules in molten $AlCl_3$ should be a rare event.

4.3. Structure and Binding Energy of $AlCl_3$, $(AlCl_4)^-$ and $(AlCl_2)^+$

The $AlCl_3$ molecule is reported from experiment [35] to be planar or nearly planar with D_{3h} symmetry and an Al-Cl bond length of 2.06 Å. Our model yields the equilibrium shape of this molecule as an equilateral triangle with an Al-Cl bond length of 2.06 Å, the binding energy being -50.6 eV relative

to separated ions. Therefore, we estimate that the dissociation reaction

$$Al_2Cl_6 \rightarrow 2(AlCl_3) \tag{4.2}$$

requires an energy expense of about 1.5 eV.

We have tested a further aspect of our model by evaluating the dissociation of Al_2Cl_6 into ionized products according to the reaction

$$Al_2Cl_6 \rightarrow (AlCl_4)^- + (AlCl_2)^+. \tag{4.3}$$

$(AlCl_4)^-$ has tetrahedral shape with an Al-Cl bond length of 2.15 Å and we estimate its binding energy as -54.2 eV. We find that $(AlCl_2)^+$ has linear shape with an Al-Cl bond length of 1.98 Å and a binding energy of -41.2 eV. Thus, the reaction in Eqn. (4.3) is estimated to require an energy expense of more than 7 eV. As one should expect, the dissociation of Al_2Cl_6 into ionized species is found to be strongly unfavoured relative to dissociation into neutral monomers.

4.4. Dissociation Path for Al_2Cl_6

We have also examined the possibility that the ionized products in Eqn. (4.3) may appear at some intermediate stage along the dissociation path of Al_2Cl_6, by being stabilized by the anion-cation Coulomb attraction over some range of finite values for the Al-Al distance $r_{Al\text{-}Al}$. This test has been carried out by determining the equilibrium structure of the Al_2Cl_6 cluster and its binding energy as functions of $r_{Al\text{-}Al}$ over a range extending from its equilibrium value of 3.22 Å (see Tab. II) up to $r_{Al\text{-}Al} = 10$ Å. At this latter value the equilibrium state of the ionic cluster consists unambiguously of two separated $AlCl_3$ monomers, although with a specific relative orientation still allowing a very tiny energy gain relative to two completely independent monomers.

Three types of molecular configurations are compared at each value of $r_{Al\text{-}Al}$: (i) a stretched configuration preserving the D_{2h} symmetry (two bridging chlorines at the same distance from both metal ions), (ii) a symmetry broken configuration representing two incipient $AlCl_3$ monomers, and (iii) a symmetry broken configuration in which both bridging chlorines are brought near one of the metal ions. The findings of these calculations are briefly as follows. For values of $r_{Al\text{-}Al}$ up to 3.7 Å the stretched symmetric configuration of the dimer is the only stable one. At $r_{Al\text{-}Al} \approx 3.7$ Å it becomes

energetically favourable for the molecule to break its symmetric shape into two incipient $AlCl_3$ monomers. However, an incipient $[(AlCl_4)^- + (AlCl_2)^+]$ configuration is still unstable up to $r_{Al\text{-}Al} \approx 4.2$ Å. Above this value of the Al-Al distance the stretched symmetric shape is energetically unstable against the incipient ionized products, but these are at much higher energy than the incipient neutral monomers.

We conclude that the dissociation of Al_2Cl_6 strictly proceeds in accord with Eqn. (4.2) and that at no stage along the dissociation path do ionized products appear as intermediate species. The conclusion from these results in conjunction with those reported in § 4.2 above is that the dimer in the dense liquid phase is strongly stable against fluctuations leading to ionic clusters carrying net charges. This result is in accord with the extremely low value of the electrical conductivity of molten aluminium trichloride as recalled in § 1.

5. VIBRATIONAL FREQUENCIES OF IONIC CLUSTERS

We have calculated the vibrational frequencies of all the ionic clusters that we have discussed in the preceding sections, using the PX_1 model in the programme that we have briefly described in § 2. The results are reported in Tables V and VI in comparison with data from infrared and Raman spectroscopy and with results from molecular orbital calculations. The spectroscopic data are from work on molten chloroaluminates [36,37] for $(AlCl_4)^-$, on solids [38] for $(Al_2Cl_7)^-$ and on the vapour [30] for Al_2Cl_6. The quantum chemical results are from work at the Hartree-Fock level (basis set 6–31G*) by Curtiss and Nichols [34] for $(AlCl_4)^-$ and by Alvarenga *et al.* [4] for Al_2Cl_6, while for $(Al_2Cl_7)^-$ in the C_2 structure they are from work carried out by Davis *et al.* [33] by a semi-empirical method. We do not consider in this context the available fits of experimental data by valence force field methods.

It is useful to recall [39] that the $(AlCl_4)^-$ tetrahedron has four independent vibrational frequencies, corresponding to normal modes whose main character may be succinctly described as (i) stretching of an Al-Cl bond as a precursor to break-up into $AlCl_3 + Cl$ (a mode conventionally denoted by ν_3), (ii) symmetric stretching of the four Al-Cl bonds (the ν_1 "breathing" mode), and (iii) deformation and torsion modes (denoted by ν_2 and ν_4). Tables V and VI refer to the two main types of stretching modes and bending modes, respectively, and follow them across the series of ionic clusters. The natural order of the modes then is that of decreasing frequency.

TABLE V Frequencies of mainly stretching modes (in cm $^{-1}$). Values in parentheses are from experiment and from molecular orbital calculations as referenced in the main text

$(AlCl_4)^-$	$(Al_2Cl_7)^-/C_2$	Al_2Cl_6	$(Al_2Cl_5)^+$	$AlCl_3$	$(AlCl_2)^+$
580 (490, 510)	674 (560, 583)	764 (625, 647)	888	767	1063
	672 (550, 576)	753 (610, 636)	874		
	642 (540, 556)	645 (501, 537)	632		
	631 (526, 551)	589 (484, 497)			
425 (351, 353)	517 (429, 448)	518 (420, 430)	603	501	586
	469 (383, 399)	417 (336, 351)	491		
	370 (336, 351)	376 (320,329)	316		
	320 (310, 320)	290 (289, 267)			

TABLE VI Frequencies of mainly deformational and torsional modes (in cm^{-1}). Values in parentheses are from experiment and from molecular orbital calculations as referenced in the main text

$(AlCl_4)^-$	$(Al_2Cl_7)^-/C_2$	Al_2Cl_6	$(Al_2Cl_5)^+$	$AlCl_3$	$(AlCl_2)^+$
196 (186, 192)	235 (226, 185)	278 (217, 232)	268	235	150
	199 (--, 172)	188 (175, 191)	260	161	
	185 (176, 164)	178 (166, 178)	200		
	172 (--, 149)	152, (144, 150)	156		
	160 (--, 145)	142 (135, 138)			
	158 (152, 138)				
117 (121, 121)	115 (--, 109)	122 (--, 126)	129		
	96 (112, 88)	110 (116, 126)	118		
	84 (--, 81)	106 (99, 102)	101		
	73 (--, 79)	58 (--, 68)	80		
	56 (--, 46)	23 (--, 23)	18		
	31 (--, 21)				
	21 (--, 7)				

5.1. Bond Stretching

As discussed by Manteghetti and Potier [38], in $(Al_2Cl_7)^-$ the splitting of the ν_d vibration of a pyramidal $AlCl_3$ group by the loss of ternary symmetry and by the coupling of the two groups gives rise to four terminal asymmetric modes at frequencies higher than that of the ν_3 mode in $(AlCl_4)^-$. Four additional stretching modes in $(Al_2Cl_7)^-$ are related to the symmetric stretching motions of the terminal groups and of the Al-Cl^B-Al bridge.

Table V reports the frequencies of what appear to be mainly stretching modes in the various ionic clusters. The above two quadruplets of stretching modes in $(Al_2Cl_7)^-$ are correlated with the two stretching modes of $(AlCl_4)^-$ and with two quadruplets of modes in Al_2Cl_6. Further correlations are

apparent with the frequencies of mainly stretching modes in the smaller ionic clusters in Table V.

The comparison between our calculated mode frequencies and the available data in Table V clearly shows that our model generally tends to overestimate the stiffness of these ionic clusters under stretching. This defect has already been reported from calculations based on the WT model [23]. However, the discrepancies from experiment decrease as one proceeds to the low-frequency modes, which are the most relevant for fluctuations in a dense liquid phase.

5.2. Deformation Modes

As again discussed by Manteghetti and Potier [38] for $(Al_2Cl_7)^-$, the higher observed deformation modes in this ionic cluster seem to be group vibration modes perturbed by the bridge bond and hence related to the ν_4 mode in $(AlCl_4)^-$. Table VI suggests correlations between the two deformation modes of $(AlCl_4)^-$ and those of $(Al_2Cl_7)^-$, Al_2Cl_6 and $(Al_2Cl_5)^+$. The last two columns report our results for $AlCl_3$ and $(AlCl_2)^+$.

We notice from Table VI that our results are in very reasonable agreement with all the available data on the deformation mode frequencies. This indicates that our model describes rather accurately all the low-frequency motions taking place in these ionic clusters around their equilibrium configurations and should therefore be useful in accounting for the relevant structural fluctuations in molten chloroaluminates.

6. CONCLUDING REMARKS

The analysis of neutron diffraction patterns by the reverse Monte Carlo method has led to a number of useful results especially for elemental liquids [40]. However, we feel that structures deduced by this method for compounds should be looked upon with great caution in cases where (i) the experimental input totally lacks information on a crucial part of the pair correlations and (ii) chemical bonding and valence saturation at intermediate range play crucial roles. This undoubtedly is the case for the textures that nature builds from the basic $(AlCl_4)^-$ tetrahedral cluster in molten chloroaluminates up to pure liquid $AlCl_3$.

We have in this work presented a classical model of ionic interactions incorporating much of the information which is available on these textures

from experiment and from *ab initio* calculations. We have used the model to demonstrate that the dimeric structure of Al_2Cl_6 is strongly stable at the appropriate stoichiometry and to highlight the role of halogen polarizability as a model for chemical bonding in stabilizing the dimer and the complex anions. It is hoped that the model will find useful application in simulation work on chloroaluminate melts.

Needless to say, in the melts the molecular species that we have examined as isolated are strongly interacting with each other and with the alkali counterions. In an ionic model such as the one that we have presented these interactions are to be constructed from the model potentials and electric fields generated by the individual ions. This will allow structural rearrangements of the clusters and fluctuations up to dissolution as may be required by free energy minimization in a dense liquid medium.

Acknowledgements

One of us (ZA) acknowledges support from the Bogaziçi University Centre for Turkish-Balkan Physics Research and Applications, from the Turkish Scientific and Technological Research Council (Tubitak) and from the University of Istanbul.

References

[1] Tosi, M. P., Price, D. L. and Saboungi, M.-L. (1993). *Ann. Rev. Phys. Chem.*, **44**, 173.
[2] Cyvin, S. J., Klaboe, P., Rytter, E. and Øye, H. A. (1970). *J. Chem. Phys.*, **52**, 2776.
[3] Hvistendahl, J., Rytter, B. E. D. and Øye, H. (1984). *Inorg. Chem.*, **23**, 706.
[4] Alvarenga, A. D., Saboungi, M.-L., Curtiss, L. A., Grimsditch, M. and McNeil, L. E. (1994). *Molec. Phys.*, **81**, 409.
[5] Torsi, G. and Mamantov, G. (1971). *Inorg. Chem.*, **10**, 1900.
[6] Boxall, L. G., Jones, H. L. and Osteryoung, R. A. (1973). *J. Electrochem. Soc.*, **120**, 223.
[7] Ubbelohde, A. R. *The Molten State of Matter* (Wiley, Chichester 1978).
[8] Harris, R. L., Wood, R. E. and Ritter, H. L. (1951). *J. Am. Chem. Soc.*, **73**, 3150.
[9] Takahashi, S., Muneta, T., Koura, N. and Ohno, H. (1985). *J. Chem. Soc. Faraday Trans. II*, **81**, 319.
[10] Biggin, S., Cummings, S., Enderby, J. E. and Blander, M. *Proc. 5th Int. Symp. Molten Salts*, ed. M.-L. Saboungi, D. S. Newman, K. Johnson and D. Inman (Electrochem. Soc., Pennington 1986), p. 81.
[11] Kameda, Y. and Ichikawa, K. (1978). *Chem. Soc. Faraday Trans. I*, **83**, 2925.
[12] Blander, M., Bierwagen, E., Calkins, K. G., Curtiss, L. A., Price, D. L. and Saboungi, M.-L. (1992). *J. Chem. Phys.*, **97**, 2733.
[13] Saboungi, M.-L., Howe, M. A. and Price, D. L. (1993). *Molec. Phys.*, **79**, 847.
[14] Badyal, Y. S., Allen, D. A. and Howe, R. A. (1994). *J. Phys.: Condens. Matter*, **6**, 10193.
[15] Saboungi, M.-L., Rahman, A. and Blander, M. (1984). *J. Chem. Phys.*, **80**, 2141.
[16] Blander, M., Saboungi, M.-L. and Rahman, A. (1986). *J. Chem. Phys.*, **85**, 3995.
[17] Saboungi, M.-L., Rahman, A., Halley, J. W. and Blander, M. (1988). *J. Chem. Phys.*, **88**, 5818.

[18] Wyckoff, R. W. G. *Crystal Structures*, vol. 2 (Interscience, New York 1964), pp 45–77.
[19] Templeton, D. H. and Carter, G. F. (1954). *Acta Cryst.*, **58**, 940.
[20] March, N. H. and Tosi, M. P. (1980). *Phys. Chem. Liq.*, **10**, 39.
[21] Tatlipinar, H., Akdeniz, Z., Pastore, G. and Tosi, M. P. (1992). *J. Phys.: Condens. Matter*, **4**, 8933.
[22] Galli, G. and Tosi, M. P. (1984). *N. Cimento D*, **4**, 413.
[23] Wang Li and Tosi, M. P. (1988). *N. Cimento D*, **10**, 1497.
[24] Cowley, R. A., Cochran, W., Brockhouse, B. N. and Woods, A. D. B. (1963). *Phys. Rev.*, **131**, 1030.
[25] Tosi, M. P. and Doyama, M. (1967). *Phys. Rev.*, **160**, 716.
[26] Brumer, P. and Karplus, M. (1973). *J. Chem. Phys.*, **58**, 3903.
[27] Busing, W. R. (1970). *Trans. Am. Crystallogr. Assoc.*, **6**, 57.
[28] Press, W. H., Teukolsky, S. A., Vetterling, W. T. and Flannery, B. P. *Numerical Recipes in Fortran* (Cambridge University Press, New York 1992), Chapter 10.
[29] Ballone, P., Andreoni, W., Car, R. and Parrinello, M. (1988). *Phys. Rev. Lett.*, **60**, 271.
[30] Chase, M. W., Davies, C. A., Downey, J. R., Frurip, D. J., McDonald, R. A. and Syverud, A. N. (1985). *J. Phys. Chem. Ref. Data*, **14**, Suppl. No. 1.
[31] *CRC Handbook of Chemistry and Physics*, ed Lite, D. R. and Frederikse, H. P. R. (CRC Press, London 1975).
[32] Curtiss, L. A. *Proc. Joint Int. Symp. Molten Salts*, ed. G. Mamantov (The Electrochemical Society, Pennington 1987), p. 185.
[33] Davis, L. P., Dymek, C. J., Stewart, J. J. P., Clark, H. P. and Lauderdale, W. J. (1985). *J. Am. Chem. Soc.*, **107**, 5041.
[34] Curtiss, L. A. and Nichols, R. *Proc. Fifth Int. Symp. Molten Salts*, ed. Saboungi, M.-L. (The Electrochemical Society, Pennington 1986), p. 289.
[35] *Landolt-Börnstein Tables*, New Series vol. 7, ed. Hellwege, K.-H. and Hellwege, A. M. (Springer, Berlin 1976), p. 16.
[36] Begun, G. M., Bosten, C. R., Torsi, G. and Mamantov, G. (1971). *Inorg. Chem.*, **10**, 886.
[37] Hvistendahl, J., Klaeboe, P., Rytter, E. and Øye, H. A. (1984). *Inorg. Chem.*, **23**, 706.
[38] Manteghetti, A. and Potier, A. (1982). *Spectrochim. Acta*, **38A**, 141.
[39] Ferraro, J. R. and Ziomek, J. S. *Introductory Group Theory* (Plenum, New York 1975).
[40] See, e.g. Tosi, M. P. (1994). *J. Phys.: Condens. Matter*, **6**, A13.